Relativistic shocks in magnetized plasmas in the context of laboratory astrophysics

Anna Grassi

Université Pierre et Marie Curie, Paris VI.
LULI, Laboratoire pour l'Utilisation des Laser Intenses, Ecole Polytechnique, Paris.
Università di Pisa.

Outline

- Introduction to laboratory astrophysics
- From astrophysics to laboratory experiments
  (Scaling laws)
- Formation of the collisionless shock for unmagnetized and magnetized plasma (Weibel Instability)
- Preliminary analysis of experimental results
- Conclusions and future works

Laboratory Astrophysics

Hydrodynamic instabilities

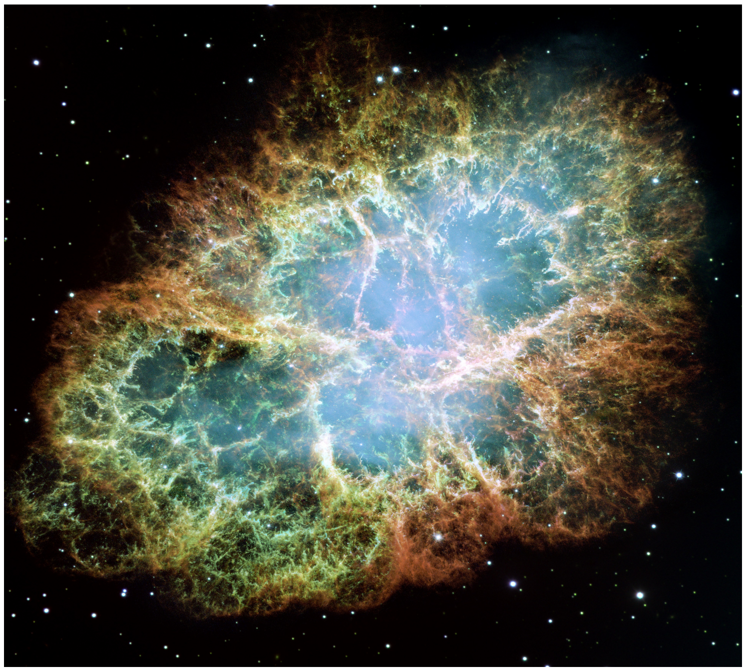

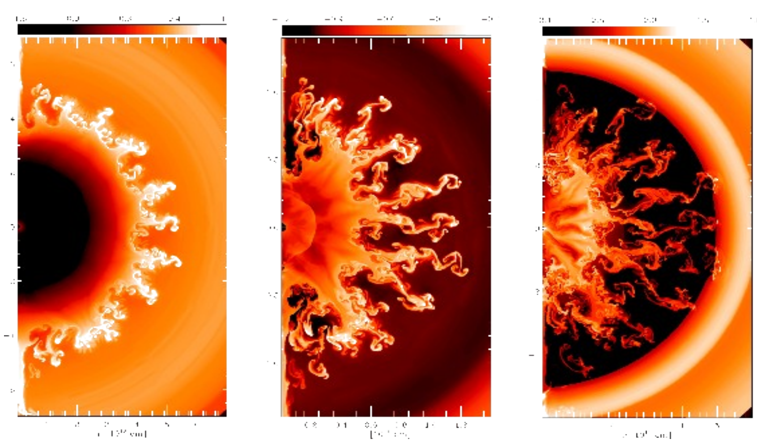

Planet interiors (Warm Dense Matter)

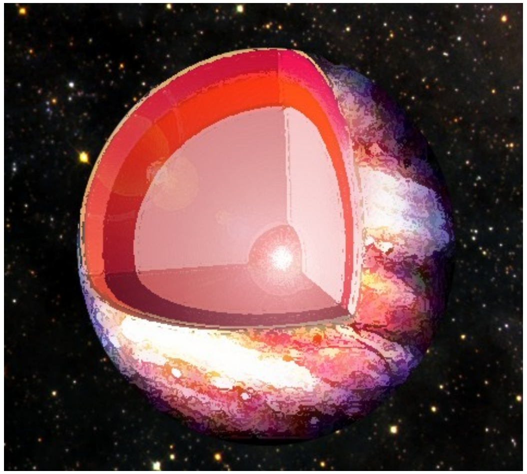

Astrophysical Jets and Shocks

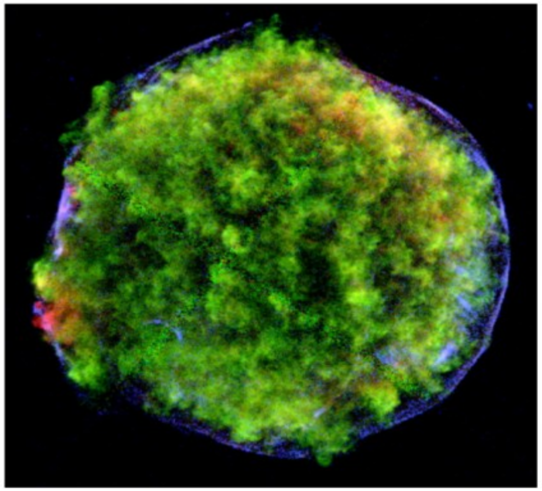

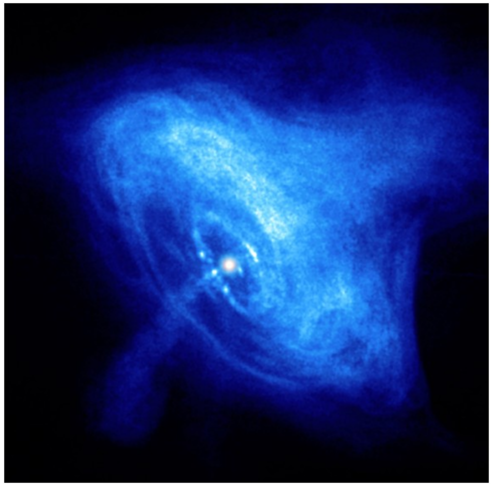

Laboratory Astrophysics

Tremendous progress in laser technology provide us with the possibility to create in the laboratory conditions resembling those of energetic astrophysical objects.

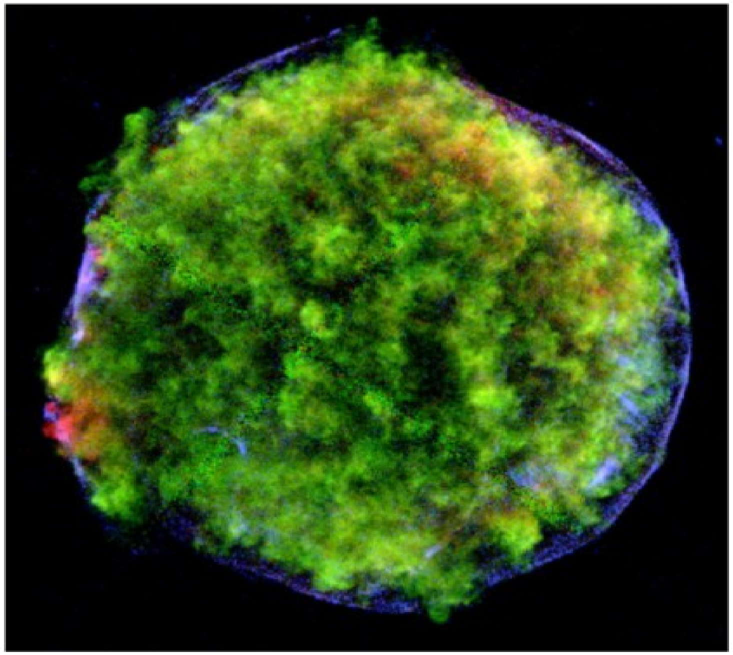

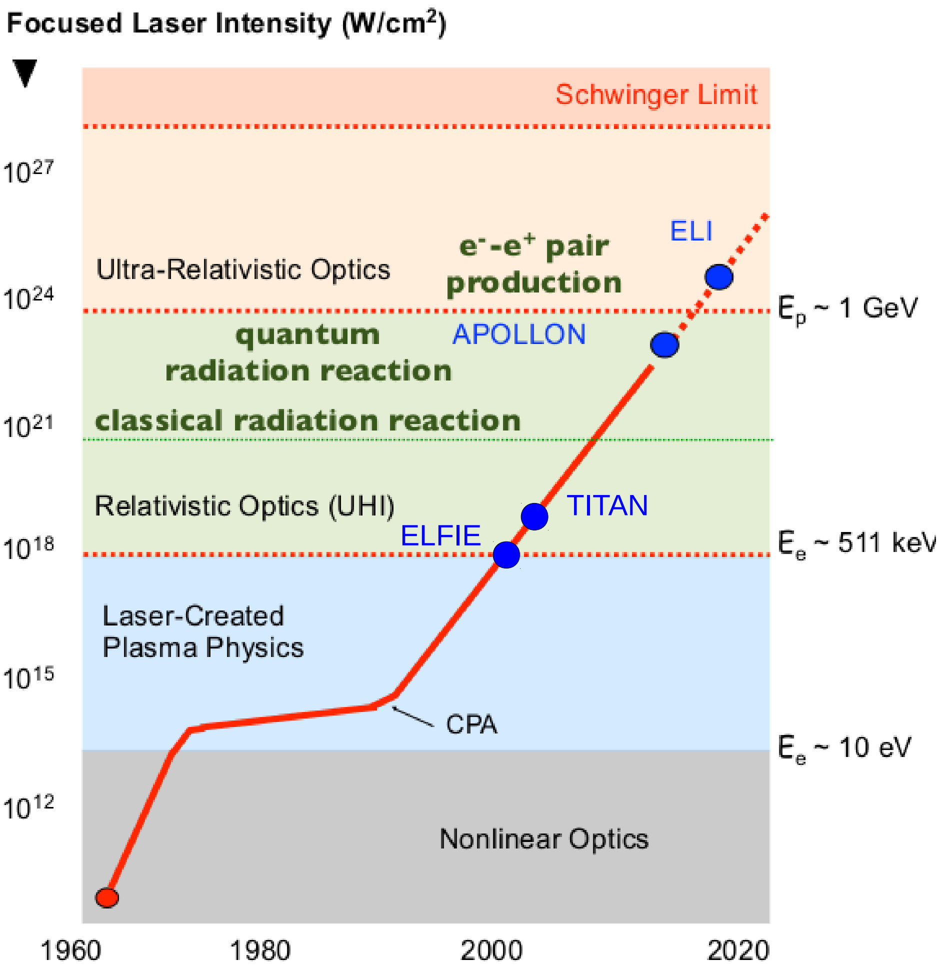

Direct access to collisionless shock waves and plasma jets :

- high-energy particles (CRs) and the resulting emission of high-energy photons
- potential production of e^+e^- pairs

Astrophysical flows and shocks often are produced in a magnetized environments,

→ laser-plasmas in strong external magnetic field

Cosmic Rays

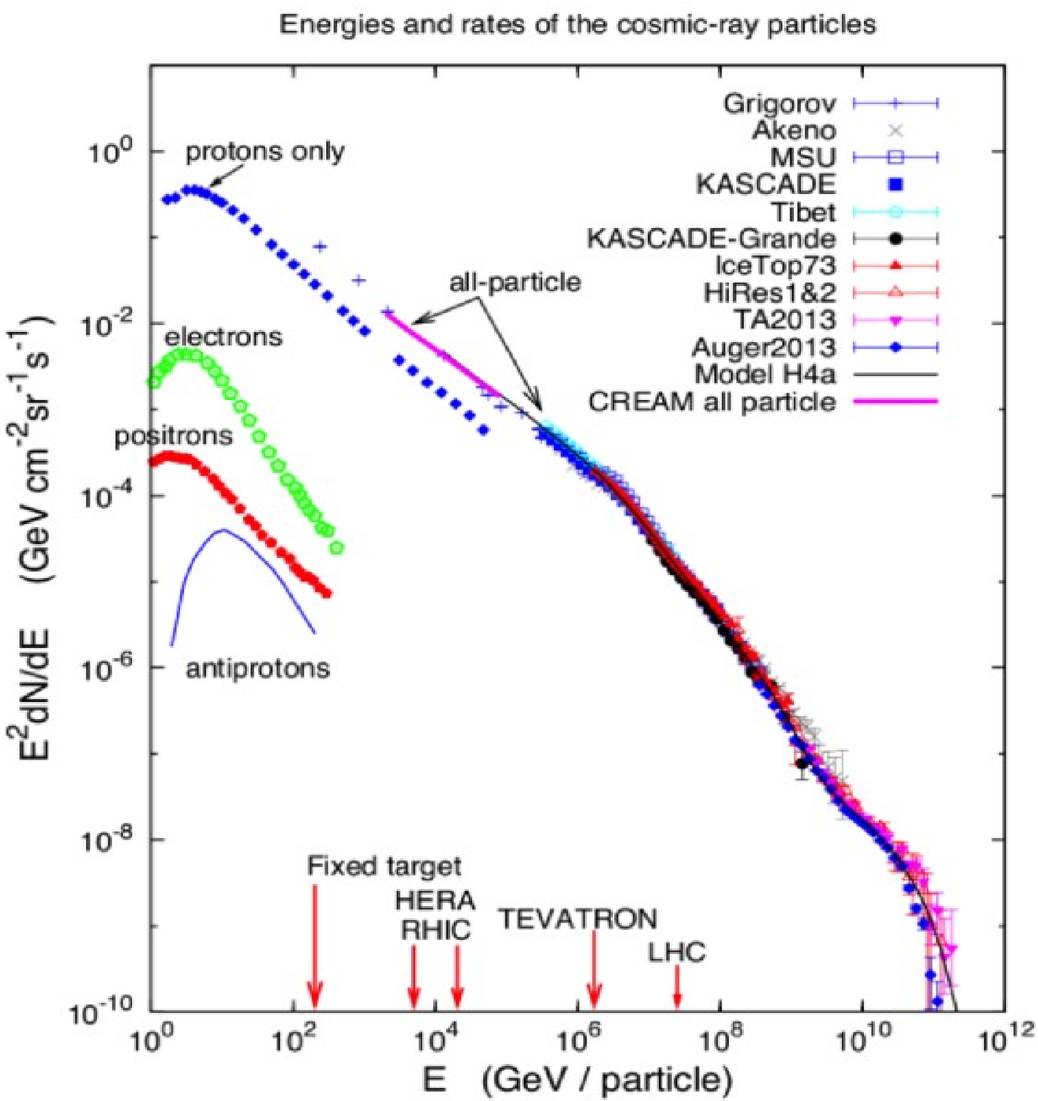

(Blasi, The origin of galactic Cosmic Rays, 2013)

Kinetic Energy at the knee

$$E_K = 3 \times 10^{15}\ \mathrm{eV}$$

Idea:
superposition of cutoffs in the spectra of different chemicals
→ Change of the slope

Acceleration Mechanism ∝ q
heavy nuclei at high energy
maximum for $E_{Fe} \sim 26 E_H$

Diffusive Shock Acceleration

Fermi Mechanism (First order) :

Particle across a collisionless shock front

$$E' = \gamma(E + pV\cos\theta)$$

$$p'_x = \gamma\left(p\cos\theta + \frac{VE}{c^2}\right)$$

After bouncing across the shock front

$$E'' = \gamma^2 E\left(1 + \frac{2Vv\cos\theta}{c^2} + \frac{V^2}{c^2}\right)$$

Average over $\cos\theta \geq 0$ ⟶ $\frac{\Delta E}{E} \propto \frac{V}{c}$

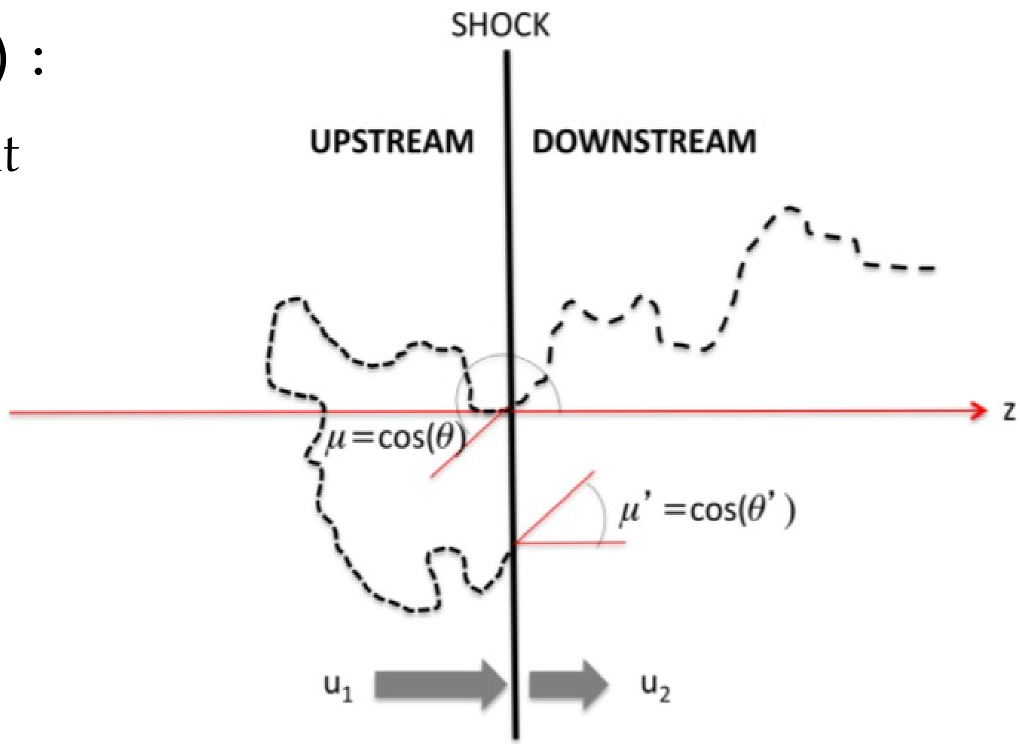

Efficiency required ~10% ⟶ necessity of non-linear effect in DSA
(Energy of the accelerated particles/Kinetic energy of the ejecta)

Injection problem : particles decoupled from thermal ones, with energy large enough to start the acceleration cycle.

SuperNova Remnants

Tycho SNR

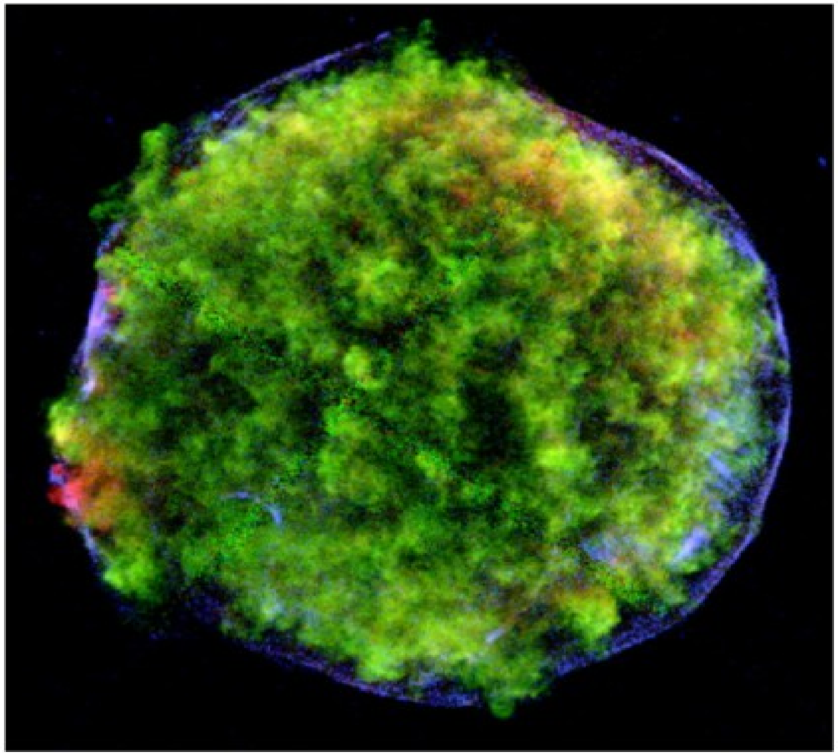

The motion of the ejecta is supersonic and drives the formation of a collisionless shock.

Evidence for CRs acceleration in SNRs

- X-ray up to 30 KeV, synchrotron radiation
  e^- up to 10 TeV, B field amplified up to ~100 μG.
- Gamma Rays emission @ 70 MeV (minimum),
  nucleon–nucleon interactions and π^0 decay.
  (Tavani et al. Astrop. J. Lett. 710, 2010)

Collisionless shock ⟶ involves a discontinuity of the macroscopic quantities on a scale length $L_{shock} \ll \lambda_{mfp}$

This abrupt change may be mediated by e.m. field (Weibel Instability)

From the astrophysical context to the laboratory experiments

Similarity criteria (MHD)

Conditions under which two systems will behave identically:

$$\partial_t \rho + \vec{\nabla} \cdot (\rho \vec{v}) = 0 \qquad \rho \frac{\mathrm{d}\vec{v}}{\mathrm{d}t} = -\vec{\nabla} p - \frac{1}{4\pi} \vec{B} \times (\vec{\nabla} \times \vec{B}) \qquad \partial_t \vec{B} = \vec{\nabla} \times (\vec{v} \times \vec{B})$$

The equations are invariant under the transformations :

$$r = a r_1 \qquad \rho = b \rho_1 \qquad p = c p_1 \quad t = a\sqrt{\frac{b}{c}} t_1 \quad v = a\sqrt{\frac{c}{b}} v_1 \quad B = \sqrt{c} B_1$$

Initial state of the two system geometrically similar

$$v(t=0) = \tilde{v} F(r/h) \qquad v_1(t_1 = 0) = \tilde{v}_1 F(r_1/h_1)$$

The similarity between the systems exists even if a shock is formed.
The Rankine-Hugoniot conditions are invariant under these transformations.

(Ryutov et al. The Astrop. J 518, 1999) (Ryutov et al. The Astrop. J. Supplement Series 127, 2000)

Example of Scaling

SuperNova 1987A after 13 years

	Astrophysical SNR	Laboratory SNR
Scale length	$L \simeq 0.03\ l.y.$	$L \simeq 100\ \mu m$
Shock front velocity	$V \simeq 10^4\ km/s$	$V \simeq 60\ km/s$
Time scale	$T \simeq 1\ y$	$T \simeq 1\ ns$
Ion density	$n_i \simeq 40\ cm^{-3}$	$n_i \simeq 5.5 \times 10^{22}\ cm^{-3}$
Magnetic field	$B \simeq 100\ \mu G$	
Localization mechanism	$r_{Li}/L \simeq 3 \times 10^{-8}$	$l_{mfp}/L \simeq 1 \times 10^{-6}$
	Magnetized plasma	Collisional plasma

Sound speed in the interstellar medium:
for typical temperatures, T ≈ 10^4 K, Cs ≈ 10 km/s.

(Ryutov et al. The Astrop. J 518, 1999) (Ryutov et al. The Astrop. J. Supplement Series 127, 2000)

Example of Scaling

SuperNova 1987A after 13 years

	Astrophysical SNR	Laboratory SNR
Scale length	$L \simeq 0.03\ l.y.$	$L \simeq 100\ \mu m$
Shock front velocity	$V \simeq 10^4\ km/s$	$V \simeq 60\ km/s$
Time scale	$T \simeq 1\ y$	$T \simeq 1\ ns$
Ion density	$n_i \simeq 40\ cm^{-3}$	$n_i \simeq 5.5 \times 10^{22}\ cm^{-3}$
Magnetic field	$B \simeq 100\ \mu G$	$B \simeq 10^5 G$
Localization mechanism	$r_{Li}/L \simeq 3 \times 10^{-8}$	

It is now possible to create high velocity magnetized plasma flows, and recover the collisionless regime.

From the Weibel instability to the collisionless shock

Weibel Instability

We consider the instability driven by two relativistic counterstreaming electron beams

The particle moving in opposite directions will concentrate in spatially separated current filaments.

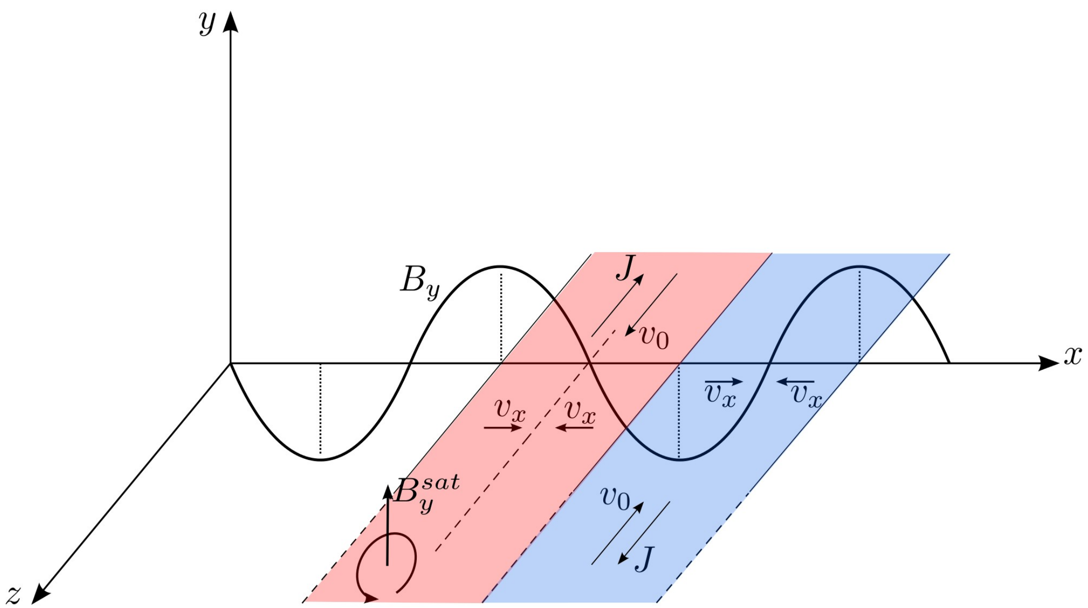

Scheme of the magnetic energy evolution

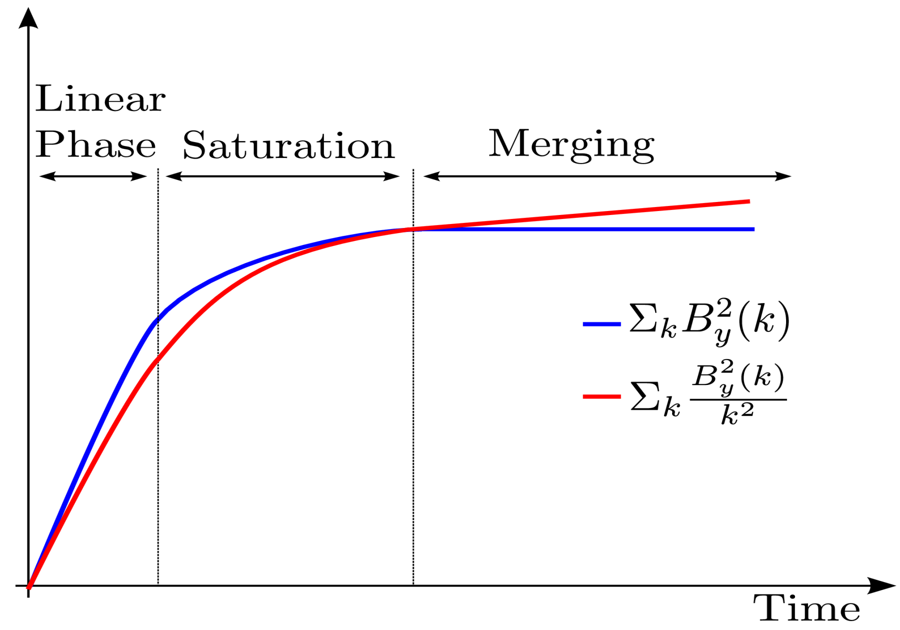

The magnetic field generated by the filaments appears to increase the initial fluctuation.

Dominant mechanisms of saturation: the Larmor radius of the particles in the growing field becomes of the order of the filament size.

(Achterberg et al. A&A 475 (2007))

Shock front formation

Symmetric counter-streaming plasma flow
Relativistic, cold and unmagnetised plasmas

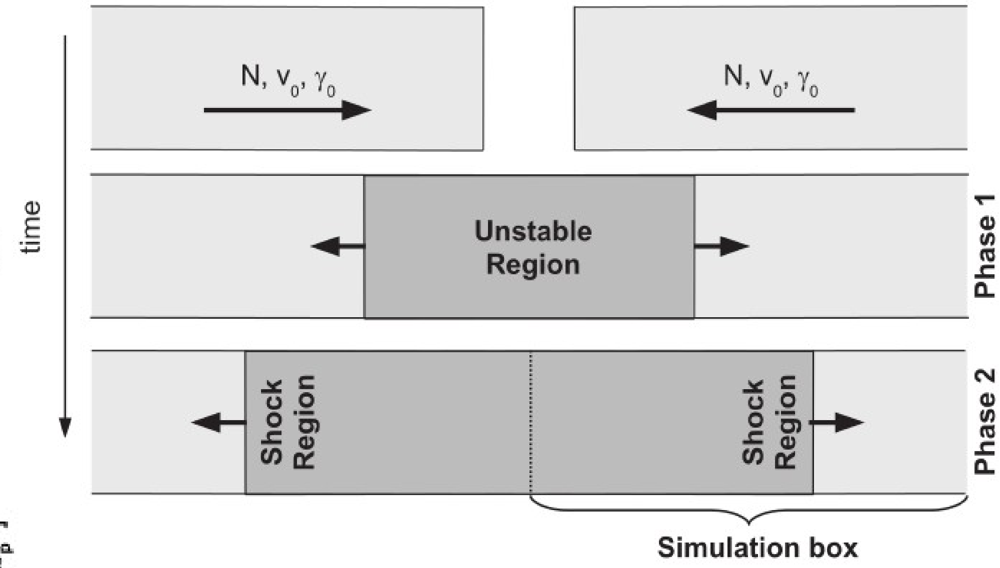

2D simulation with pair plasma with $\gamma_0 = 25$
(Bret et al. Phys. Plasmas 20, 2013)

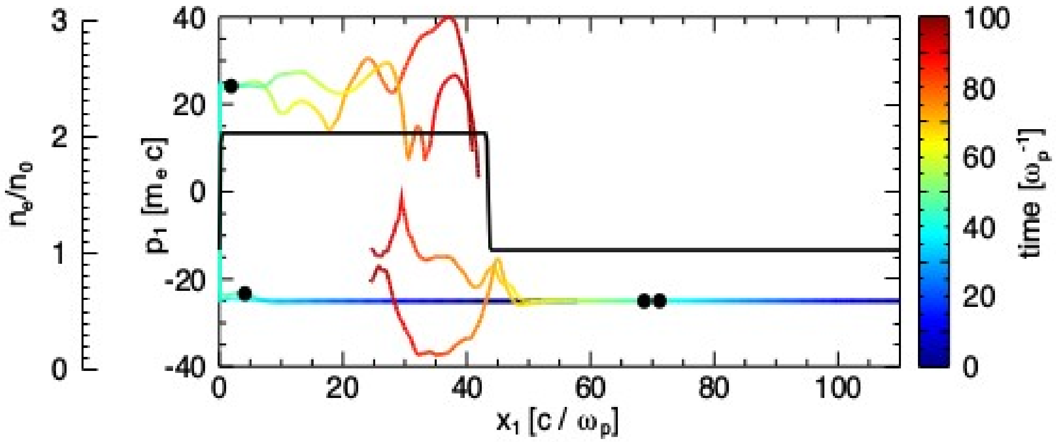

From the R.H. conditions
The required density jump in 2D

$$\frac{n_d}{n_0} = 3$$

(Bret et al. Phys. Plasmas 21, 2014)

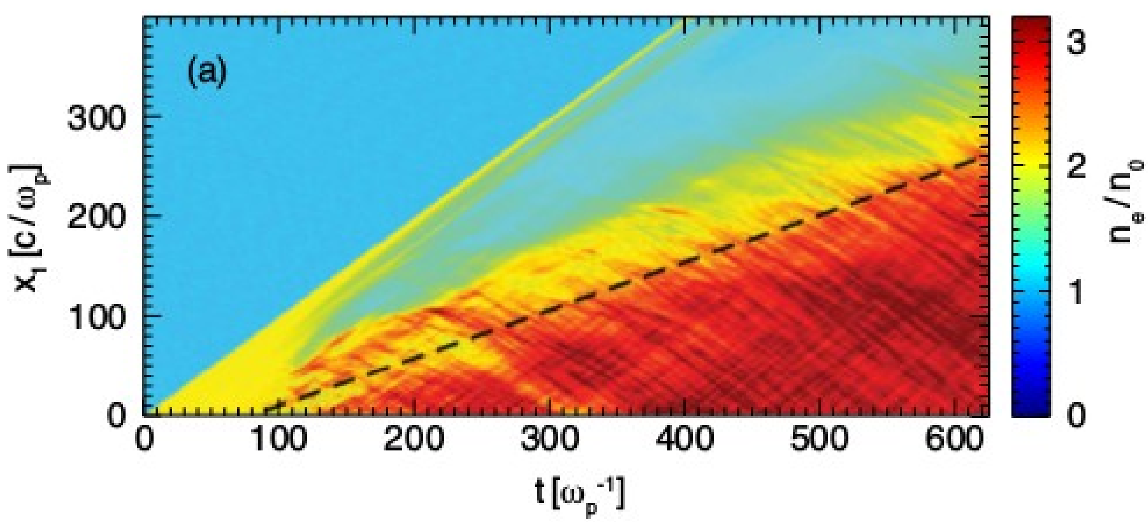

Shock front formation

Symmetric counter-streaming plasma flow
Relativistic, cold and unmagnetised plasmas

(Stockem et al. Astrop. J. Lett. 803, 2015)

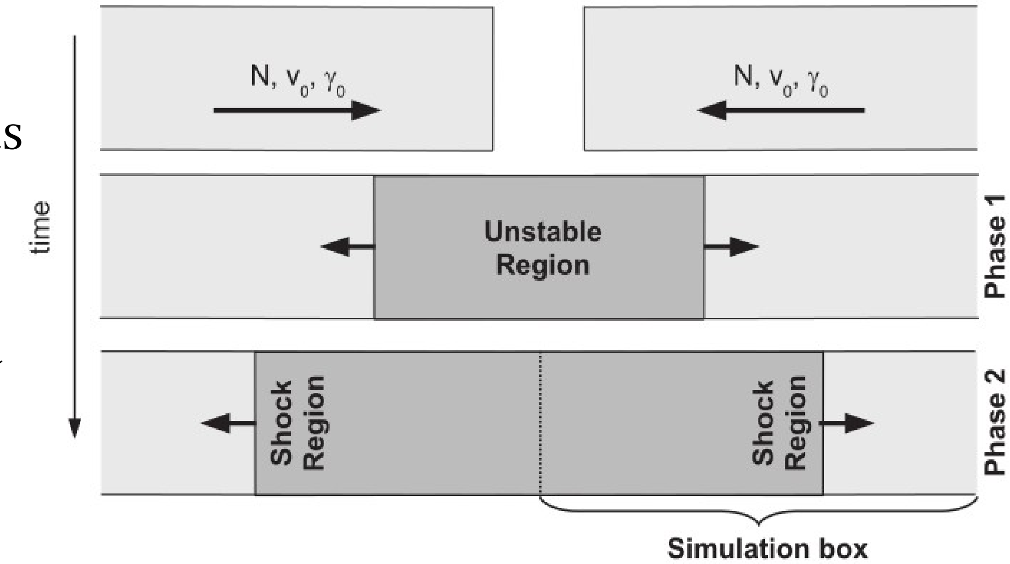

2D simulation with electron-proton plasma with $\gamma_0 = 25$

Saturation of the electron Weibel (growth rate $\omega_I \propto \omega_{pe}$) → Filaments of size ~$r_{L,e}$ as seeds for the ion Weibel

Saturation of the ion Weibel (growth rate $\omega_I \propto \omega_{pi}$)

\+

Merging of the current filaments

$$\tau_0 = 2^{3/2}\sqrt{\gamma}\omega_{pi}^{-1}.$$

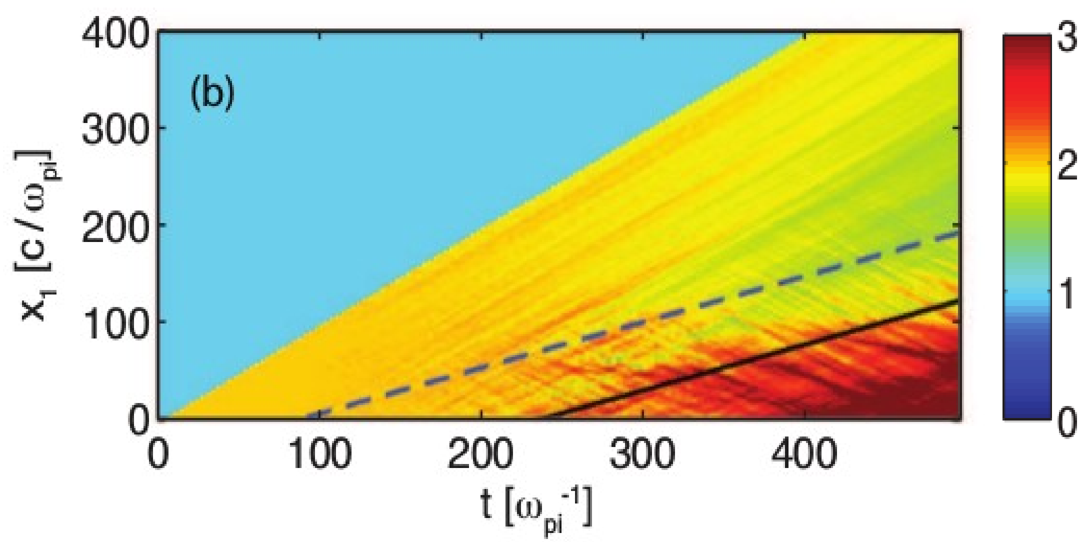

Linear phase

Analytic calculation of the growth rate:

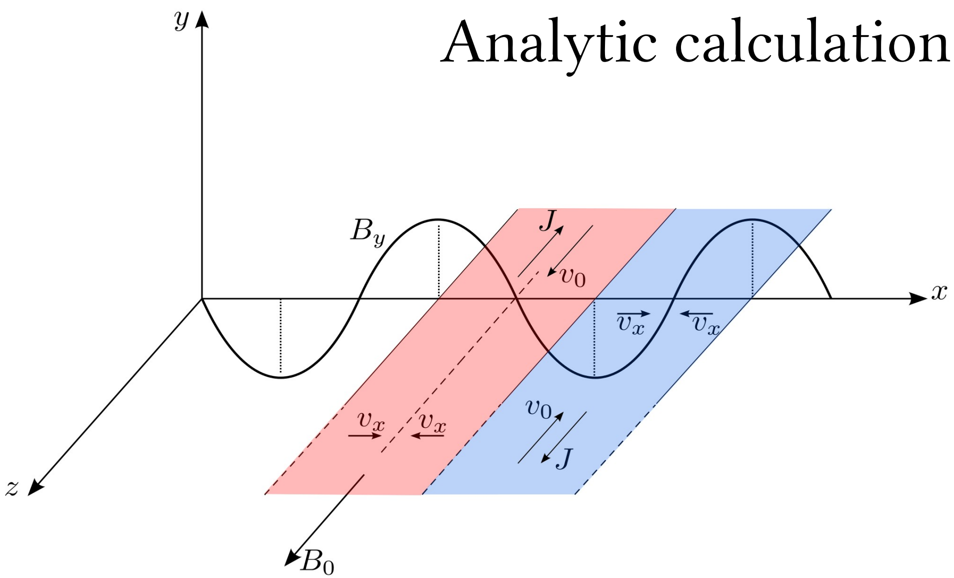

- The growth rate decreases
- Existence of a minimum unstable k
- All the purely transverse modes are stable for

$$B_0 > B_{max} = \sqrt{\gamma}\frac{v_0}{c}\frac{m_e\omega_p}{e}$$

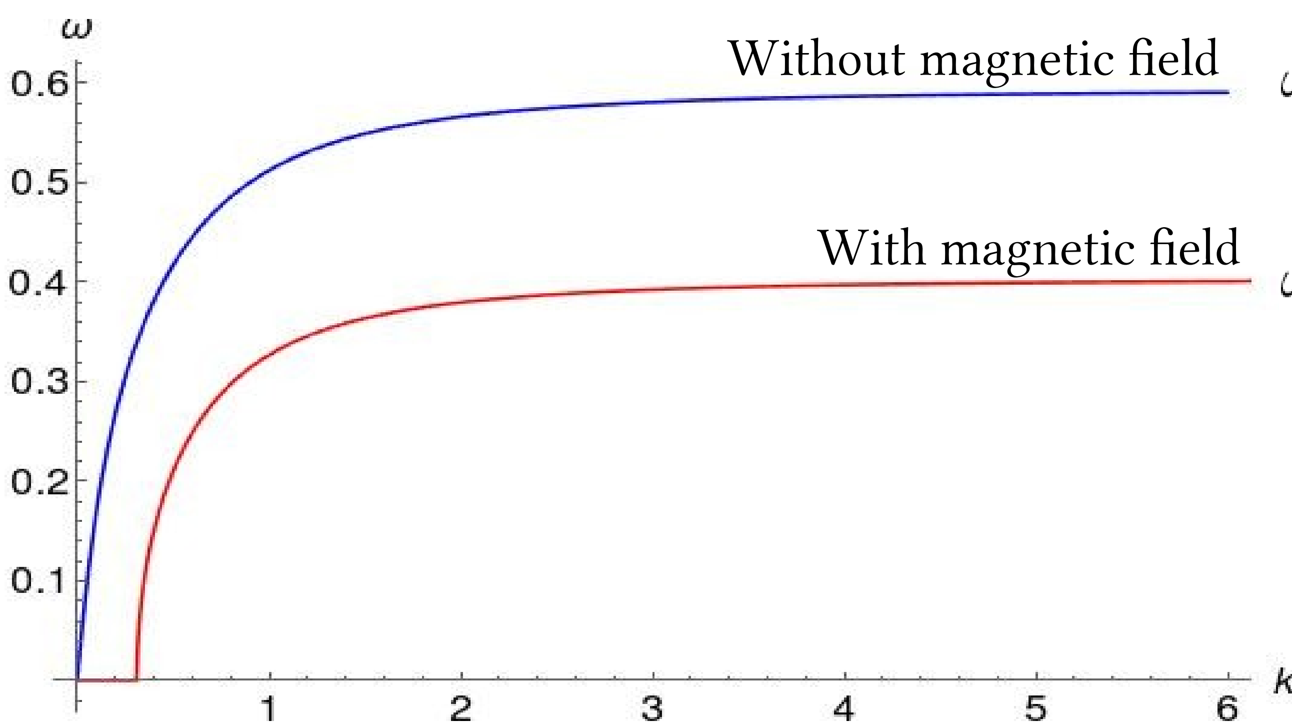

Without magnetic field $\omega_I^2 \simeq \frac{v_0^2}{c^2}\frac{\omega_p^2}{\gamma_0}$

With magnetic field $\omega_I^2 \simeq \frac{v_0^2}{c^2}\frac{\omega_p^2}{\gamma_0} - \Omega^2$

Linear phase

Analytic calculation of the growth rate:

Simulations in 1D configuration
$$\begin{cases} \partial_y = \partial_z = 0, \text{ so } \vec{k} = k_x \hat{x}. \\ B_y(t=0) = \varepsilon sin(kx) \quad \varepsilon = 10^{-3} \end{cases}$$

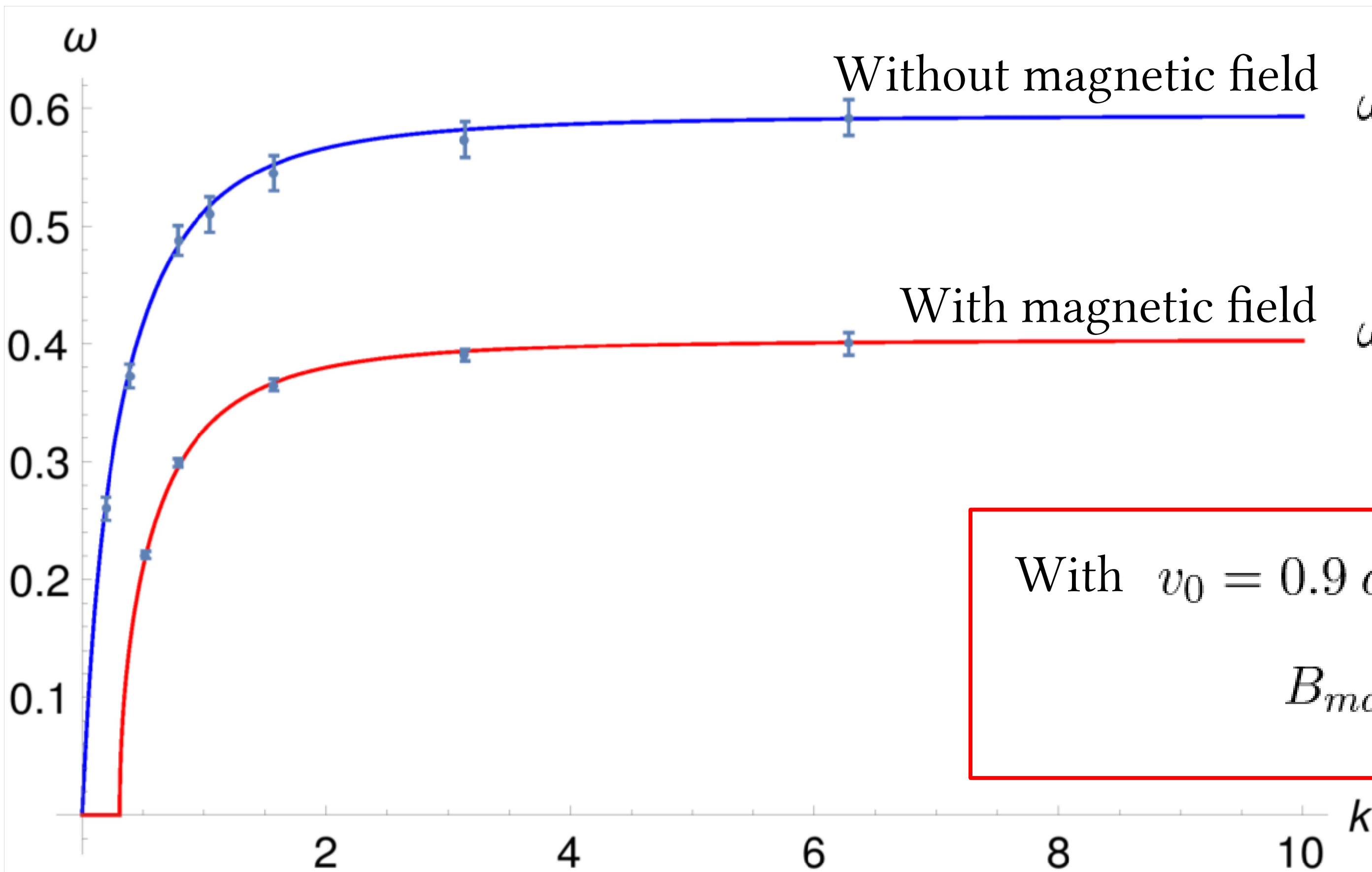

Without magnetic field
$$\omega_I^2 \simeq \frac{v_0^2}{c^2}\frac{\omega_p^2}{\gamma_0}$$

With magnetic field
$$\omega_I^2 \simeq \frac{v_0^2}{c^2}\frac{\omega_p^2}{\gamma_0} - \Omega^2$$

With $v_0 = 0.9\, c$ and $n_e = 10^{18} \text{cm}^{-3}$

$$B_{max} \simeq 4.3 \text{ T}$$

Non-linear phase

Dominant mechanisms of saturation:

The Larmor radius of the particles in the growing field equates k^{-1}

(Achterberg et al. A&A 475 (2007))

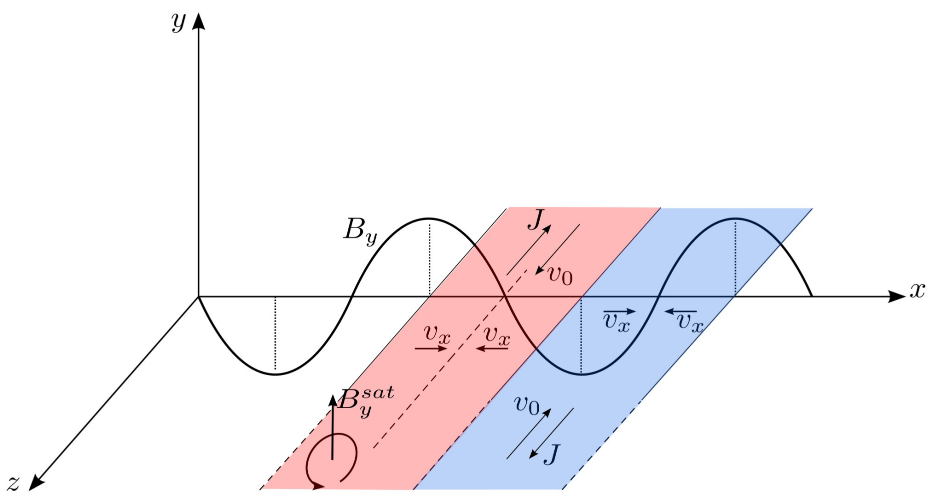

Increasing B0

- The energy density of By is redistributed to smaller scales
- The required time for merging increases

Evolution of By(k)

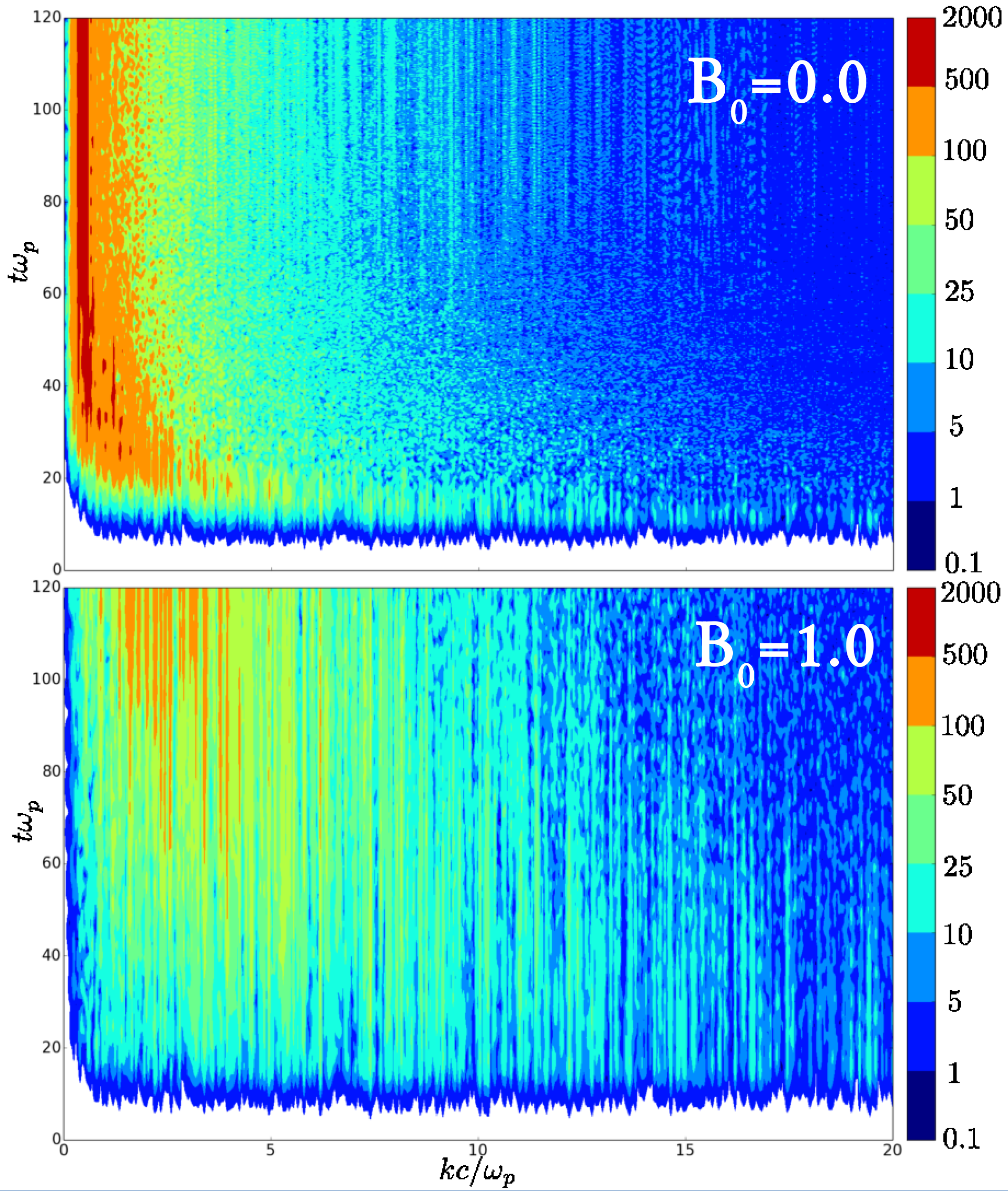

Non-linear phase

Filament merging without an external magnetic field

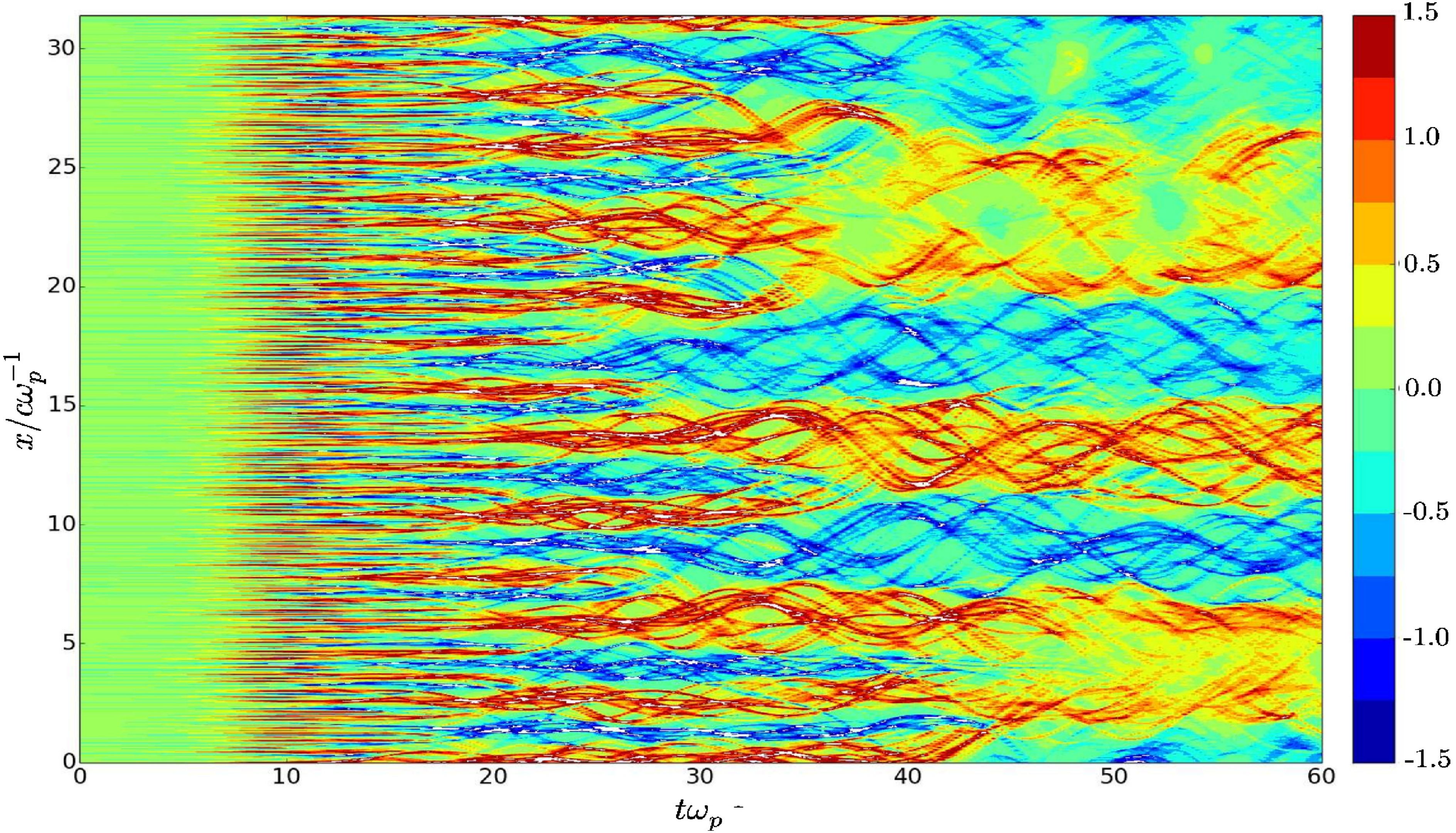

Non-linear phase

Filament merging with an external magnetic field

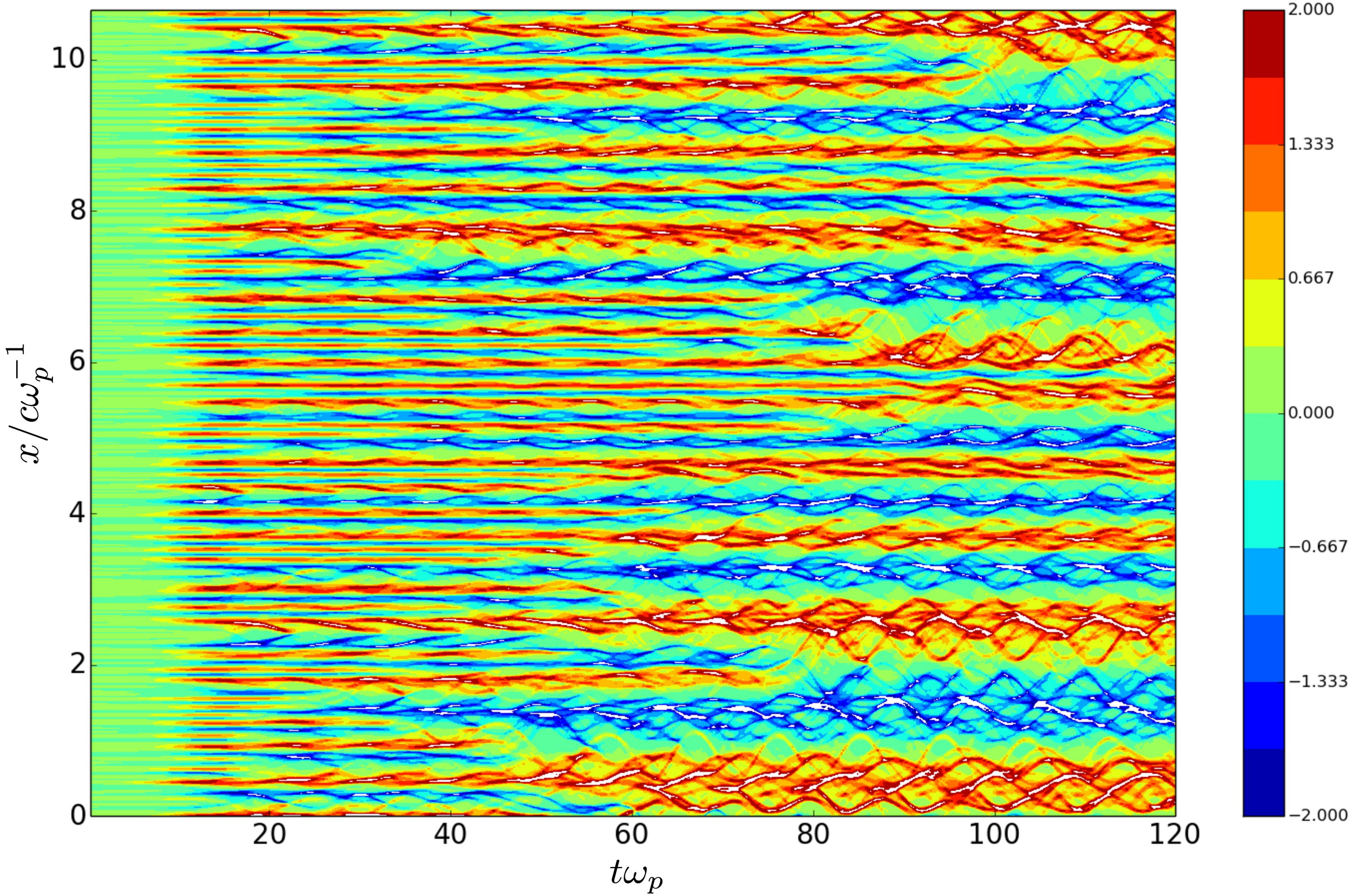

Preliminary analysis of experimental results

Titan Experiment

Collision of two high velocity magnetized plasma flows

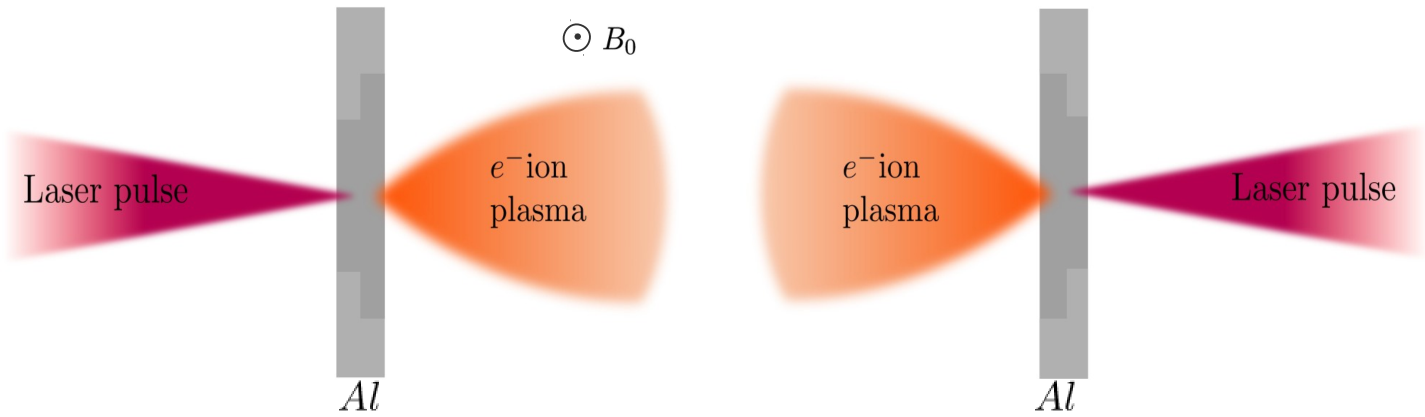

Titan Laser : 60 J/beam , 650 fs , I~5 10^{19} W/cm^2

Protons accelerated in TNSA mechanism
up to 20 MeV (β up to 0.2)

Al foil: 4.5 µm, separation 250 µm

B-field transverse to the plasma flow
Constant at 20 T within 2% up to 3 mm for 50 µs

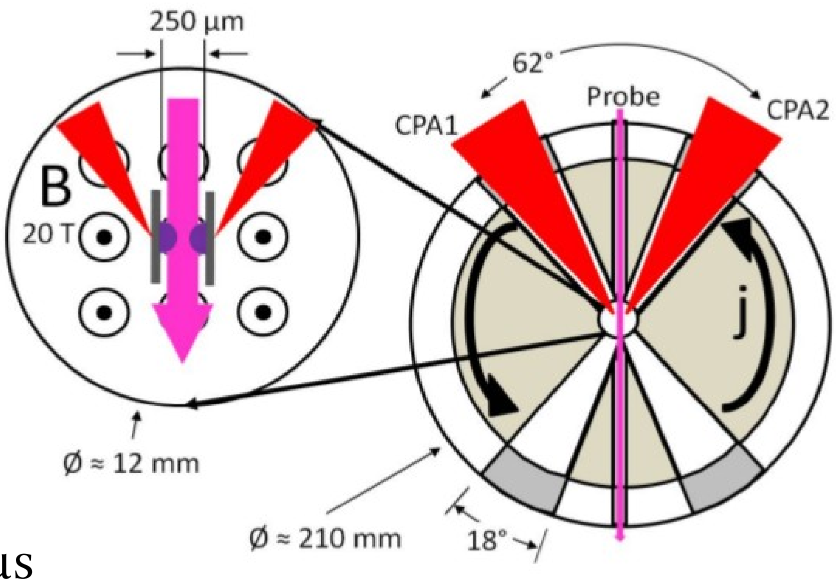

(Higginson et al. High En. Dens. Phys. , 2014)

Titan Experiment

Collision of two high velocity magnetized plasma flows

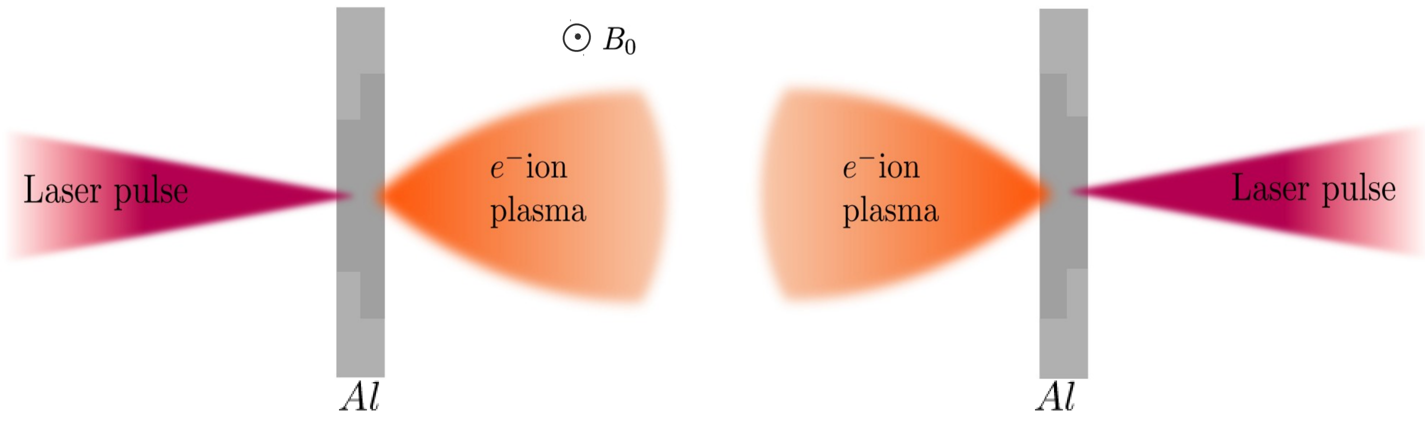

Only in the case with the external magnetic field.
Development of a density bump between 15-60 ps

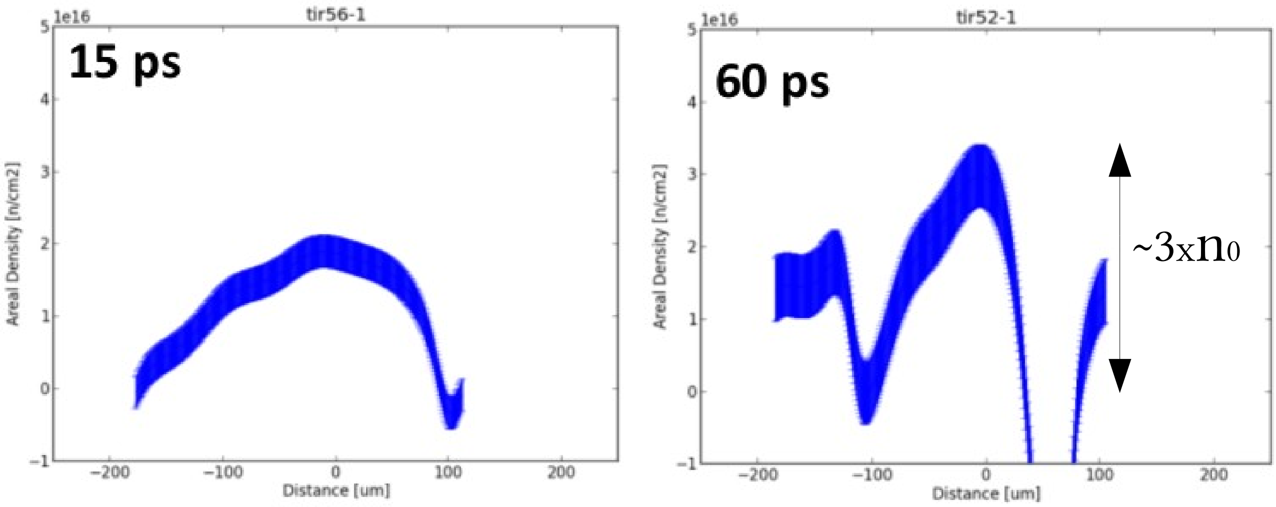

This density structure may be attributed to the generation of high magnetic field, transverse to the plasma flow, that may slow down drastically the particles

Titan Experiment

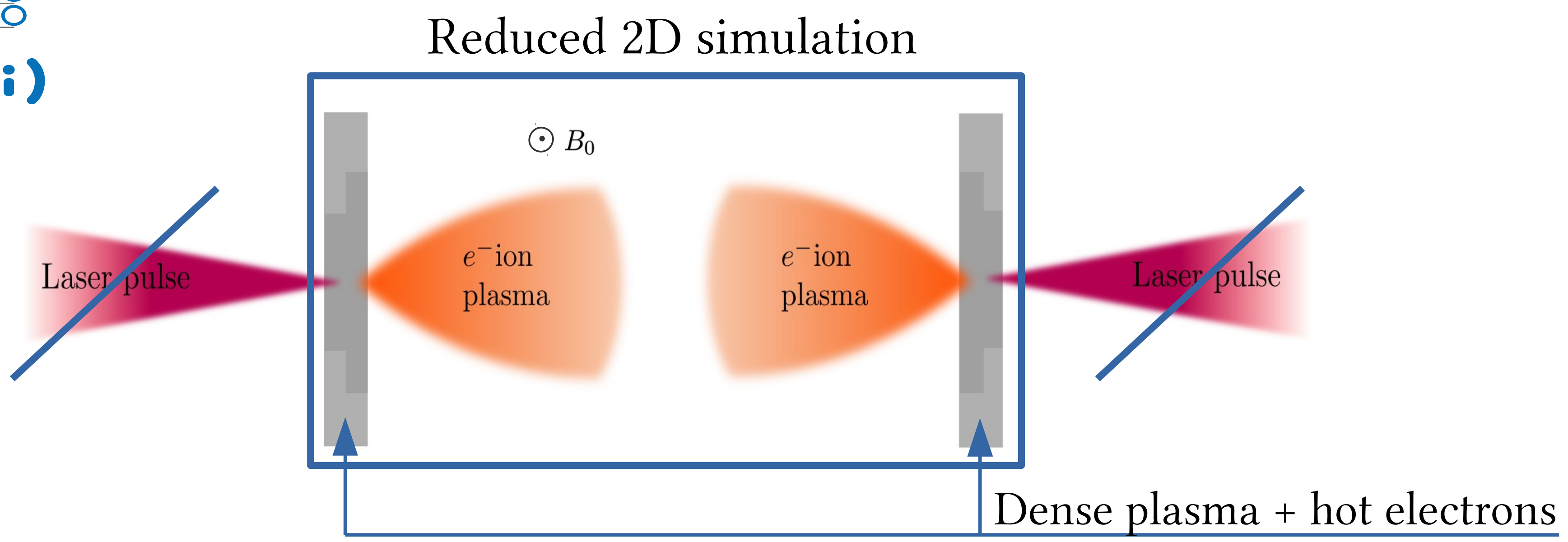

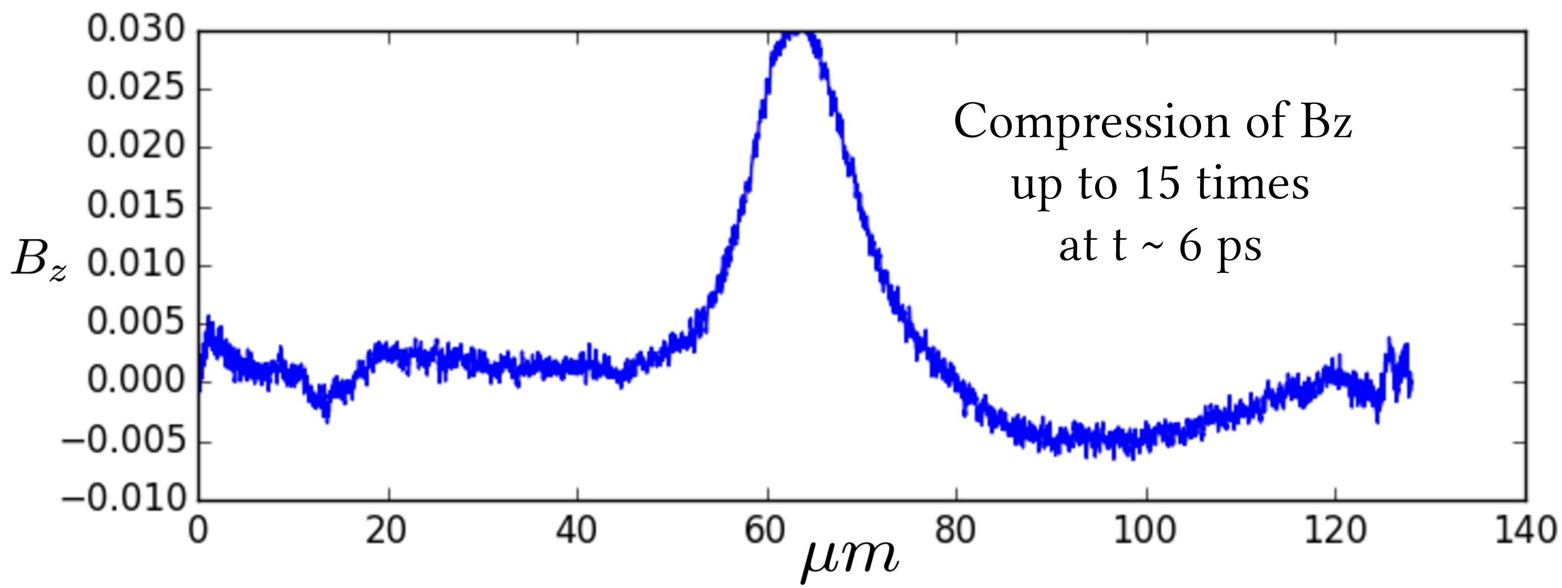

Conclusions

- Weibel Instability in magnetized plasma;
  we highlight the main difference between the case with/without magnetic field in the linear and saturation phase.

- TITAN experiment preliminary results:
  this setup should be extremely useful to enhance our understanding of collisionless shock generation and how the co-penetration of fast plasma flows may be affected by external magnetic fields.

Thanks for the attention !

Particle-In-Cell code

SMILEI (Simulating Matter Irradiated by Light at Extreme Intensities)

Open-source Particle-In-Cell code developed in C++

1D3V and 2D3V cartesian geometry

Resolution of a system of differential equations to compute the trajectories of the macro-particles

$$\frac{dx_n}{dt} = \frac{p_{x,n}}{m\gamma_n}$$

$$\frac{d\vec{p}_n}{dt} = q(\vec{E} + \frac{\vec{v}_n}{c} \times \vec{B})$$

Resolution of the Maxwell's equations to compute the e.m. fields (external fields + self-consistent fields)

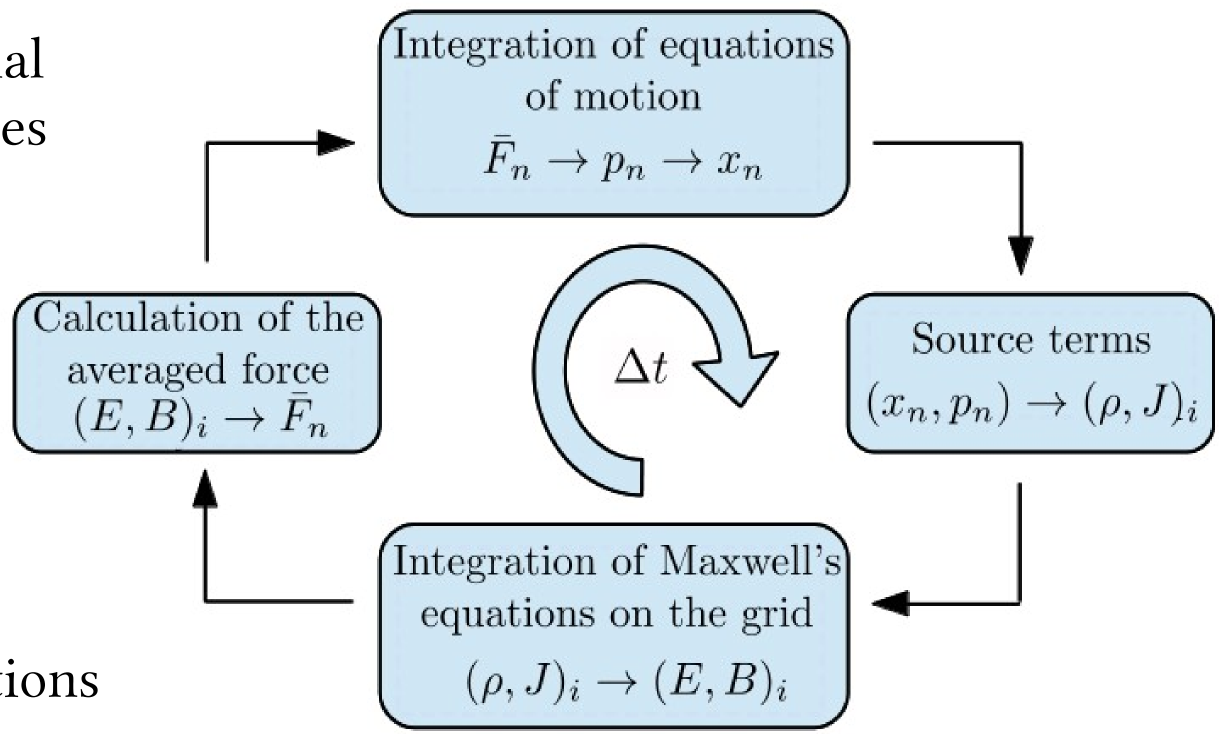

TNSA scheme

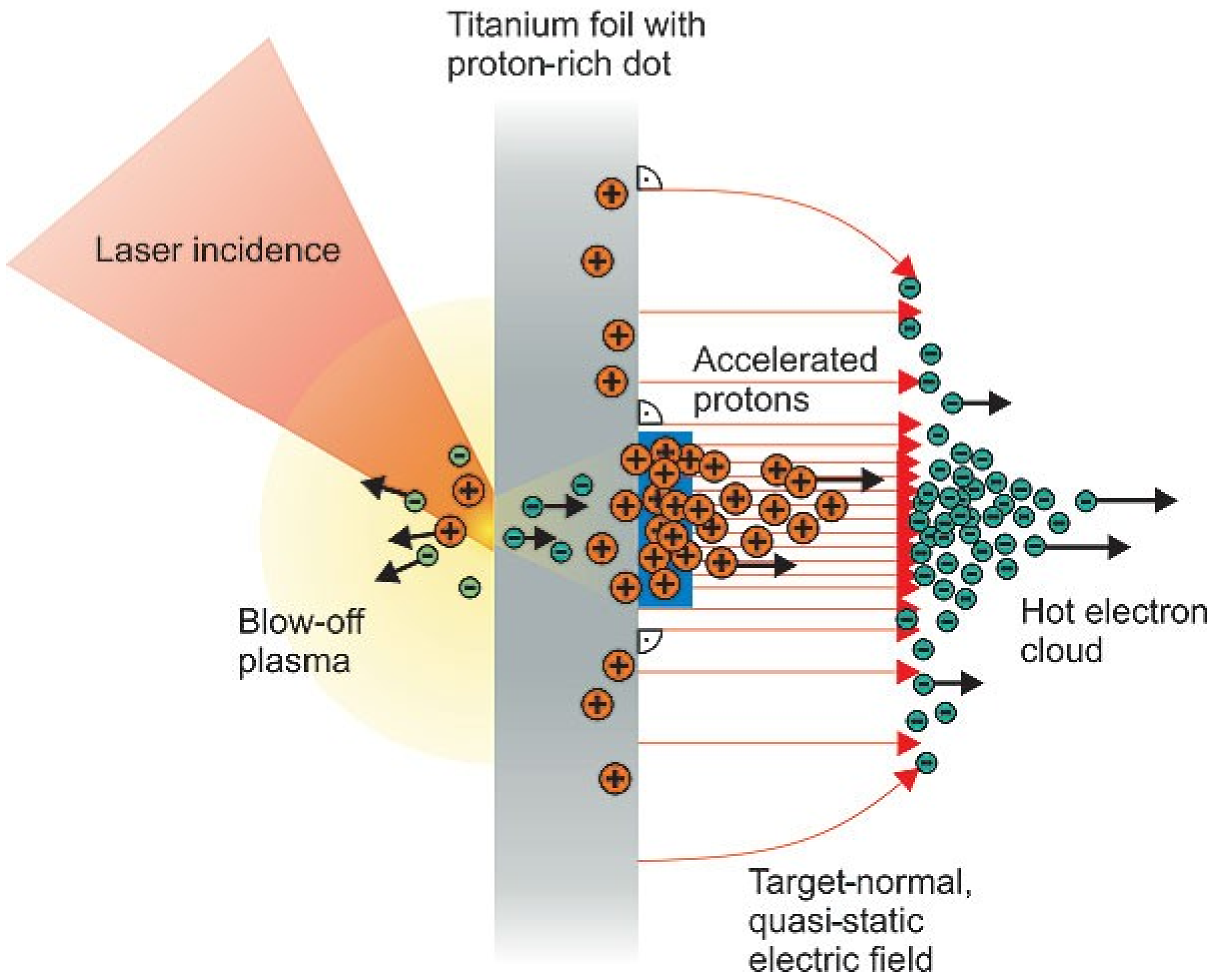
Titanium foil with
proton-rich dot
Laser incidence
Accelerated
protons
Blow-off
plasma
Hot electron
cloud
Target-normal,
quasi-static
electric field

CPA scheme

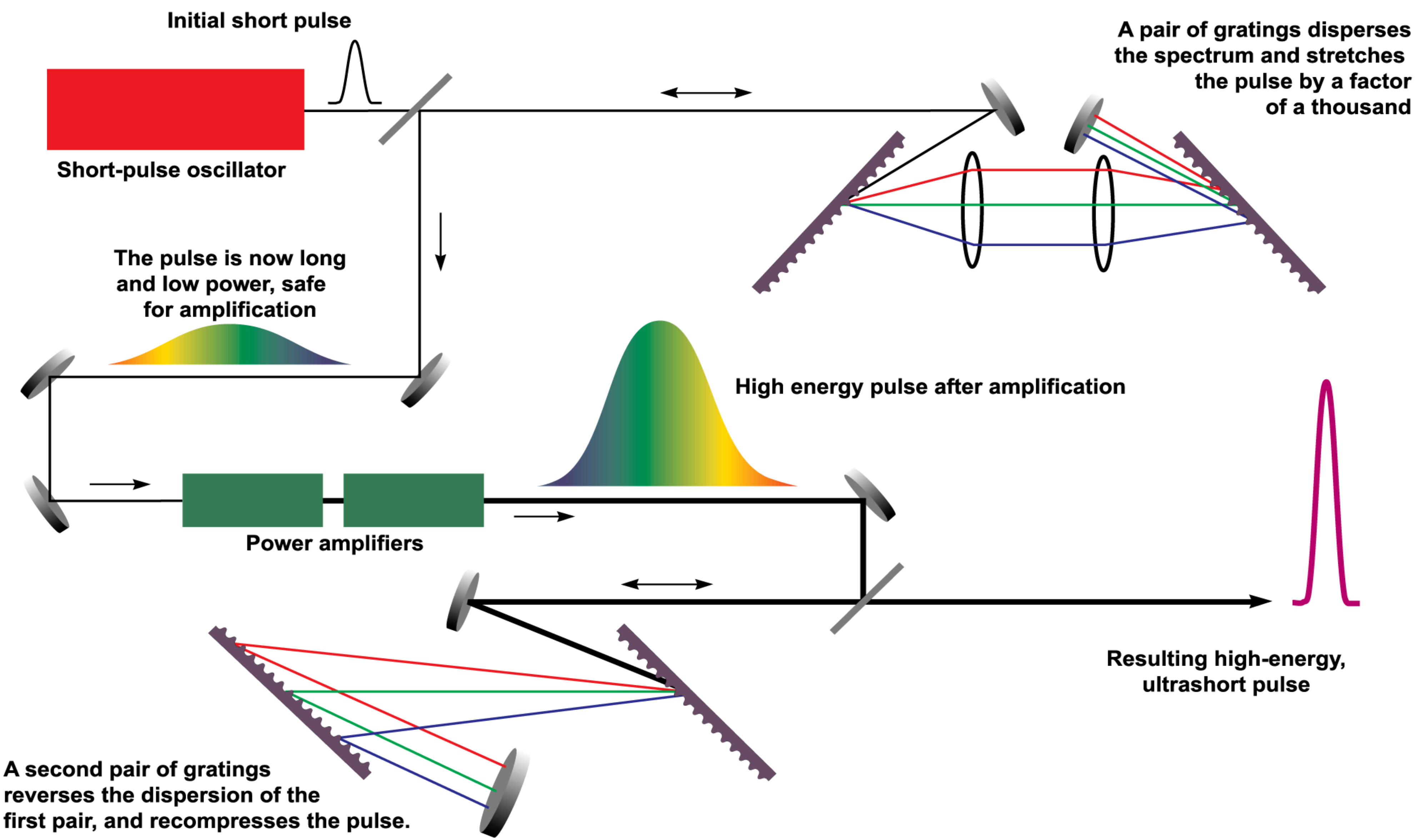
Initial short pulse
Short-pulse oscillator
A pair of gratings disperses the spectrum and stretches the pulse by a factor of a thousand
The pulse is now long and low power, safe for amplification
High energy pulse after amplification
Power amplifiers
Resulting high-energy, ultrashort pulse
A second pair of gratings reverses the dispersion of the first pair, and recompresses the pulse.